# SIMULATION OF INTENSE PROTON BEAMS IN NOVEL ISOCHRONOUS FFAG DESIGNS

S. L. Sheehy*, ASTeC/STFC, Harwell, Oxon, UK
C. Johnstone, Fermilab, Batavia, IL, U.S.A.
M. Berz, K. Makino, Michigan State University, East Lansing, MI, U.S.A.
P. Snopok, Illinois Institute of Technology, Chicago, IL, U.S.A.

## Abstract

Recent developments in the design of non-scaling fixed field alternating gradient (FFAG) accelerators have been focused on achieving isochronous behaviour with a small betatron tune excursion. These advances are particularly interesting for applications requiring CW beams, such as Accelerator Driven Systems for energy generation or waste transmutation. The latest advances in lattice design have resulted in a 330 MeV to 1 GeV lattice, isochronous to better than +/- 1%. This paper reports on simulations of recent lattice designs incorporating 3D space charge effects.

## INTRODUCTION

New FFAG designs approaching isochronicity give a tantalising possibility of providing CW beams from a strong focusing accelerator. Such an accelerator should be able to support high power beams using a constant RF frequency and fixed field magnets. CW machines have intrinsic advantages in supporting high power beams as they have a much lower peak current than a pulsed or cycling machine. It has also been speculated that due to the strong focusing nature of these accelerators, particular space charge effects may be reduced when compared to a cyclotron [1], particularly at injection where vertical focusing in a cyclotron is typically weak [2].

This work presents two FFAG designs [3], the first is a four cell design which is isochronous to $\pm 3\%$ and the other a six cell design which has now achieved isochronicity to better than $\pm 1\%$. For reasons discussed later, the four cell design is taken to be representative of this type of accelerator in the simulations presented.

### FFAG Lattice Designs

The lattice designs presented here are based on the idea of using alternating gradient magnets, incorporating a nonlinear radial field expansion with an appropriate magnet edge angle [4]. This means that the orbit at each momentum can be made proportional to velocity in order to achieve isochronicity and at the same time the betatron tune can be controlled through both edge and weak focusing.

This is in contrast to a classical cyclotron where the main field is predominantly the dipole field, which has limitations in adapting the path length to velocity into the relativistic regime. It should be noted that a modern design of a sector cyclotron may in fact look very similar to these

recent FFAG designs and in some cases the distinction between the type of accelerator begins to blur [5]. For the purposes of this work we will refer to the designs as FFAGs as this indicates that the lattice design consists of 'F' and 'D' magnets which are opposite in field polarity, meaning that the 'D' magnet provides a reverse bend. Each lattice is completely periodic and in each magnet the radial field has a carefully defined gradient and the magnets have linear edge profiles.
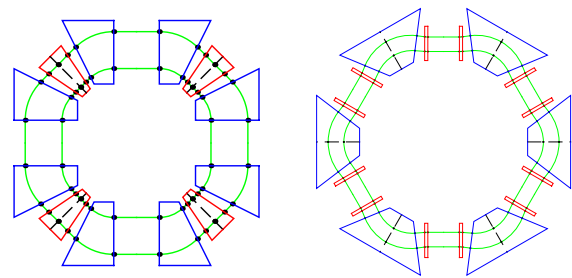


Figure 1: Layout of the 4 cell ring (left) and 6 cell ring (right).

### 4-cell FFAG Design

The four cell ring is completely periodic and uses a triplet FDF cell structure. A minimum 0.3 - 0.5 m length has been imposed between magnets to prevent end-field overlap and cross talk between magnets. The long straight is 2 m to accommodate injection, extraction and the acceleration cavities.

A four-cell ring periodicity was found to be a strong initial starting point and isochronous to +/-3% over an energy range from 0.25-1 GeV. The ring parameters are given in Table 1. Note that a complete CW accelerator system would likely entail an H- injector. (Use of H- in the lower energy ring permits CW injection into the higher-energy ring through charge-changing or stripping methods.)

### 6-cell FFAG Design

The six cell ring uses a DFD cell structure, which produces a smaller horizontal beta function and beam size at extraction and is thus preferred. This design is isochronous to +/-1% over its proposed energy range. The choice of a slightly higher injection energy was informed by developments of smaller injector rings, which have a wider range of applications in medical and other areas at 330 MeV rather than 250 MeV.

---

* suzie.sheehy@stfc.ac.uk

Table 1: General Parameters, 4-cell 1 GeV FFAG

| Parameter | 250 MeV | 585 MeV | 1000 MeV |
|---|---|---|---|
| Avg. Radius [m] | 3.419 | 4.307 | 5.030 |
| $\nu_x/\nu_y$ (cell) | 0.380/0.237 | 0.400/0.149 | 0.383/0.242 |
| Field F/D [T] | 1.62/−0.14 | 2.06/−0.31 | 2.35/−0.42 |
| Magnet Size F/D [m] | 1.17/0.38 | 1.59/0.79 | 1.94/1.14 |

Table 2: General Parameters, 6-cell 1 GeV FFAG

| Parameter | 330 MeV | 500 MeV | 1000 MeV |
|---|---|---|---|
| Avg. Radius [m] | 5.498 | 6.087 | 7.086 |
| $\nu_x/\nu_y$ (cell) | 0.297/0.196 | 0.313/0.206 | 0.367/0.235 |
| Field F/D [T] | 1.7/−0.1 | 1.8/−1.9 | 1.9/−3.8 |
| Magnet Size F/D [m] | 1.96/0.20 | 2.79/0.20 | 4.09/0.20 |

In this instance the 'D' magnets are significantly shorter than the 'F' magnet and the rapid azimuthal variation in field has proved problematic in advanced simulations which rely on interpolation of a midplane field map. This issue is being addressed with developments in the OPAL Framework [6]. As such, space charge simulations have been performed using the four cell design as it is representative of this general type of accelerator. In addition, the four cell design is the more compact of the two, so one would expect any effects to be more pronounced than in the six cell case.

## SPACE CHARGE

Due to the small gap and relatively large width of the magnets in these designs, both the direct and image space charge tune shifts must be considered. The direct space charge tune shift if the beam were truly CW can be estimated assuming an un-bunched round beam and the indirect contribution is calculated for a round beam between parallel conducting walls assuming that the beam pipe half height, $g$ and the magnet half-gap $h$ are 0.025 m.

$$\Delta Q_x = -\frac{r_0 R}{\beta} \left( \frac{N}{\gamma^2 L} \left[ \frac{1}{2\epsilon_n} - \frac{\pi^2 \langle \beta_x \rangle}{24\beta\gamma h^2} \right] - \frac{N_{tot}\pi\langle\beta_x\rangle}{24\beta\gamma R}\left(\frac{1}{2h^2}+\frac{\beta^2}{g^2}\right)\right) \quad (1)$$

$$\Delta Q_y = -\frac{r_0 R}{\beta} \left( \frac{N}{\gamma^2 L} \left[ \frac{1}{2\epsilon_n} + \frac{\pi^2 \langle \beta_x \rangle}{24\beta\gamma h^2} \right] + \frac{N_{tot}\pi\langle\beta_x\rangle}{24\beta\gamma R}\left(\frac{1}{2h^2}+\frac{\beta^2}{g^2}\right)\right). \quad (2)$$

Where $L$ is the machine length ($L = 2\pi R$), and $\epsilon_n$ is the normalised emittance. The direct and indirect tune shift

contributions for this design at 300 MeV and 1 GeV are given in Table 3.

Table 3: Contributions to Estimated Space Charge Tune Shift Assuming a 10 mA CW Beam with a $10\,\pi$ mm mrad Emittance

| | | **Direct** | **Indirect** |
|---|---|---|---|
| $\Delta\nu_x$ | 300 MeV | 1.85 x $10^{-3}$ | +1.604 x $10^{-4}$ |
| $\Delta\nu_y$ | 300 MeV | 1.85 x $10^{-3}$ | -1.891 x $10^{-4}$ |
| $\Delta\nu_x$ | 1 GeV | -2.686 x $10^{-4}$ | +6.496 x $10^{-5}$ |
| $\Delta\nu_y$ | 1 GeV | -2.686 x $10^{-4}$ | -7.662 x $10^{-5}$ |

In reality a beam is not perfectly CW but has some sub-structure depending on injection scenario and the chosen RF harmonic. In any case, the purely CW direct tune shifts are negligible, so in simulating this machine with space charge, a single bunch is used as a 'worst-case scenario' of only injecting a single bunch per turn. The intensity can then be increased which will raise the peak current to the point where space charge effects become interesting.

The four cell mid-plane field map is imported into the OPAL Framework and a $10\,\pi$ mm mrad (un-normalised) matched beam is tracked for 50 turns at both 300 MeV and 500 MeV with a parabolic beam distribution. The single bunch is around 80 cm long with a uniform profile, thus filling around 3.7% of the ring. Simulations are run with average currents varying from 0 mA up to 100 mA, which corresponds to a peak current of up to 2.73 A if a single bunch per turn is assumed. At the 100 mA level there are 7.19 x $10^{10}$ particles in the bunch with a total bunch charge of 11.52 nC, which obviously scales with the average current. The emittance evolution throughout the 50 turns is shown in Fig. 2 and Fig. 3. Note that the emittance growth effects are negligible with a realistic average beam current of around 10 mA, even in the worst-case scenario of a single bunch per turn.

RF acceleration is not included in the simulations and the longitudinal bunch is able to grow depending on the space charge forces. For the most part, this growth in length is only small. If we take the direct space charge tune shift to be significant, say $\delta\nu$ = -0.2, the corresponding peak current to create that tune shift is around 11 A. For a single bunch which takes up 3.7% of the ring as before, this is equivalent to 8.04 x $10^{12}$ particles per pulse and an average current of around 400 mA. In this case a slightly more realistic parabolic longitudinal beam profile is adopted, but otherwise with the same parameters as before. The results of 20 turns at 300 MeV are shown in Fig. 4 and the spatial distributions are shown in Fig. 5.

In this case the longitudinal bunch length growth is significant and while this is far above the required operational beam current of 10 mA, the effects of very high currents in these machines is an interesting topic in itself. It should be noted that as this machine is cyclotron-like there is no longitudinal focusing from RF and there is strong coupling of
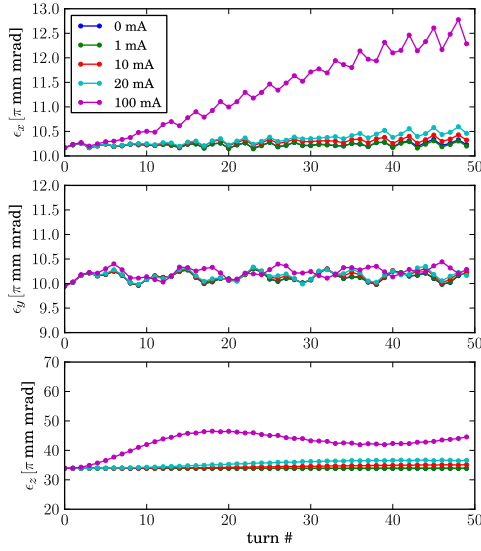
Figure 2: Emittance evolution in 50 turns at 300 MeV with varying average beam current, for horizontal (top), vertical (middle) and longitudinal (lower).
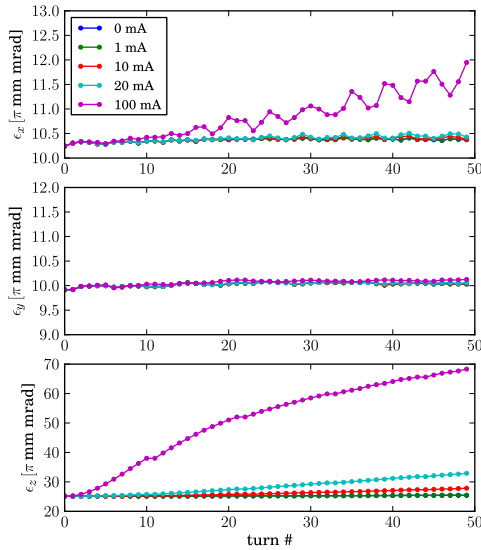




Figure 3: Emittance evolution in 50 turns at 500 MeV with varying average beam current, for horizontal (top), vertical (middle) and longitudinal (lower).

Figure 4: Horizontal (left) and longitudinal (right) phase space at 0° of a 300 MeV parabolic beam at turn 0, 1, 2, 5, 10 and 20 showing bunch length growth with increased beam current. Blue is 0 mA and red is an average current of 400 mA. At high intensity the beam grows longitudinally from $\pm 0.4\,m$ to $\pm 0.6\,m$.

the motion in the longitudinal and radial direction. Future studies will incorporate RF and acceleration to study these space charge effects in more detail.

## DISCUSSION

One of the major unanswered questions in these designs is the extraction mechanism. There are a number of extrac-
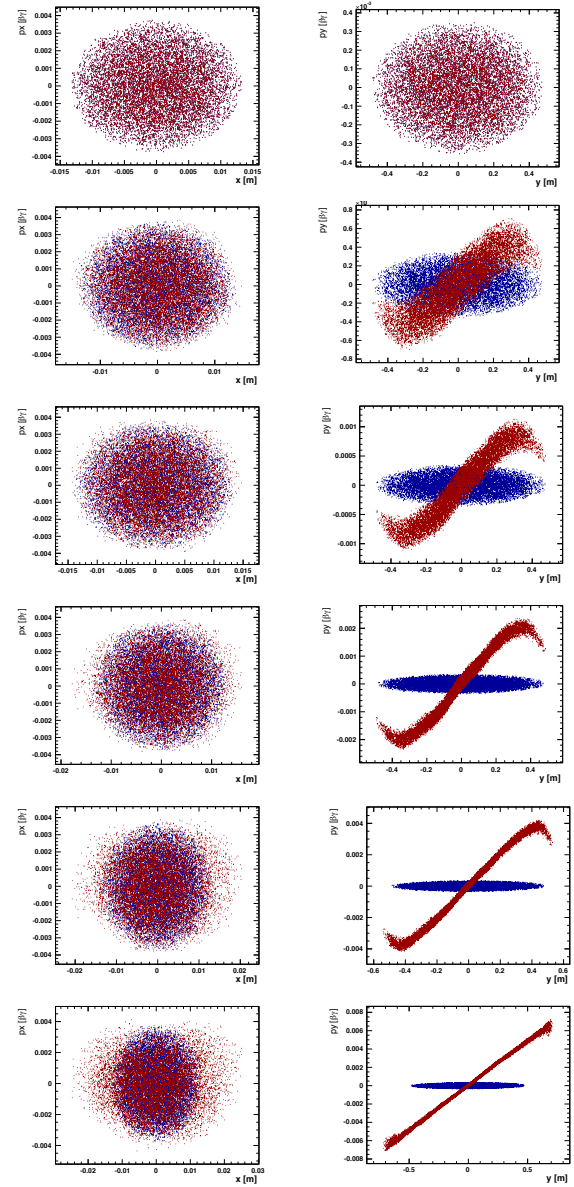
tion options for medium to high energy cyclotron-like machines including resonant and non-resonant extraction [7]. Some techniques are more applicable to high intensity accelerators than others, as beam loss is a major concern. Most likely, the intensity limit of the machine will be determined by longitudinal space charge limits and beam loss.

Without an unrealistically large energy gain per turn, simply using acceleration to create a turn separation and extract through an electrostatic or electromagnetic channel seems unlikely. Some enhancement of the turn separation
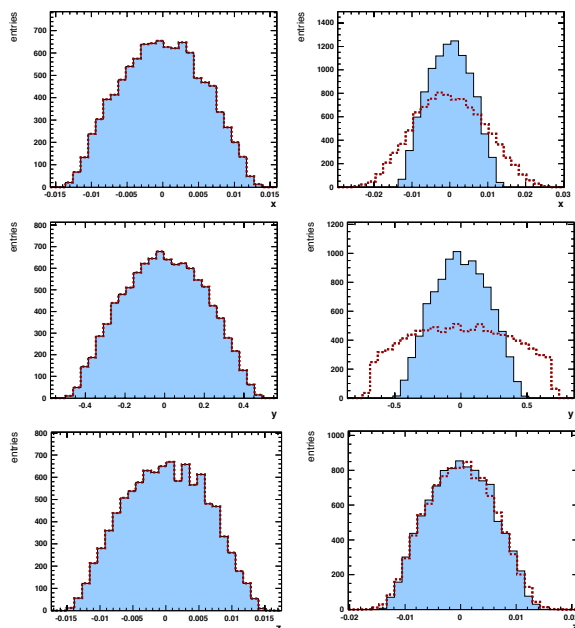
Figure 5: Horizontal, longitudinal and vertical 1D distributions of a 300 MeV parabolic beam at turn 0 (left) and 20 (right) with 0 mA beam (blue) and a 400 mA beam (red dash) which corresponds to a peak current of around 11 A.

through the use of resonances will most likely be required. For this, there are a number of options depending on the choice of resonance; integer, half integer, higher order resonances and so on have all been considered in cyclotrons and some higher order resonances have also been considered in FFAGs [8]. A similar study is an item of future work for these designs.

## ACKNOWLEDGMENT

## REFERENCES

[1] C. Johnstone, M. Berz, K. Makino, S. Koscielniak, P. Snopok, Int. Journal Modern Physics A 26 (2011) 1690-1712.

[2] Th. Stammbach *et al.*, Nucl. Instrum. Meth. B 113 (1996), p. 1-7.

[3] C. Johnstone, P. Snopok, F. Meot, Proceedings of the International Particle Accelerator Conference, New Orleans, 2012, p. 4118-4120. http://www.JACoW.org

[4] C. Johnstone, *et al.*, Proceedings of the 19th International Conference on Cyclotrons and Their Applications, Lanzhou, China, 2010, p. 389-394. http://www.JACoW.org

[5] R. Baartmann, Private Communication, 2012.

[6] A. Adelmann *et al.*, "The OPAL (Object Oriented Parallel Accelerator Library) Framework", PSI-PR-08-02, Paul Scherrer Institut (2008).

[7] W. Joho, Proceedings of the 5th Int. Conf. on Cyclotrons, Butterworths, London (1871), p. 159.

[8] T. Yokoi, Int. Journal Modern Physics A 26 (2011) p. 1873-1886.